doi.org/10.32426/engresv9n6-001

Engineering Research

Technical Reports

Volume 9 – Issue 6 – Article 1

ISSN 2179-7625 (online)

ANALYSIS OF THREE-PHASE SVPWM MICROCONTROLLED INVERTER WITH FOCUS ON HARMONICS GENERATION

Luiz C. Gomes[1], Francisco J. Grandinetti[2], Márcio A. Marcelino[3], Giorgio E. O. Giacaglia[4], Wendell de Q. Lamas[5]

NOVEMBER / 2018

Taubaté, São Paulo, Brazil

[1] Graduate Program in Mechanical Engineering, Department of Mechanical Engineering, University of Taubaté, englcgomes@gmail.com.
[2] Graduate Program in Mechanical Engineering, Department of Mechanical Engineering, University of Taubaté; and Department of Mechanical Engineering, São Paulo State University at Guaratinguetá, fjgrandinetti@hotmail.com.
[3] Graduate Program in Mechanical Engineering, Department of Mechanical Engineering, University of Taubaté; and Department of Electrical Engineering, São Paulo State University at Guaratinguetá, abud@feg.unesp.br.
[4] Graduate Program in Mechanical Engineering, Department of Mechanical Engineering, University of Taubaté, giacaglia@gmail.com.
[5] Lorena School of Engineering, University of São Paulo, wendell.lamas@usp.br.

Engineering Research: Technical Reports

The “Engineering Research” is a publication with purpose of technical and academic knowledge dissemination.

ANALYSIS OF THREE-PHASE SVPWM MICROCONTROLLED INVERTER WITH FOCUS ON HARMONICS GENERATION

Abstract. *This work presents SVPWM modulation technique concepts in a simple and direct way, aiming at the level of harmonics generated measurement, in order to evaluate its performance and to compare with another method of modulation widely used and known as SPWM. It also presents the generation algorithm, implemented and simulated in an 8-bit microcontroller. PWM is a technique used by inverters to control induction motors, aiming to control rotation and torque. Several techniques have been developed, the most famous being SPWM, due to its simplicity and performance, and the most recent being SVPWM, which has gained the confidence and preference of designers, mainly due to its performance characteristics. A bibliographic study was necessary to implement the SVPWM with simulations in EXCEL, PSIM, MATLAB and PROTEUS for a better understanding of the algorithm concepts and construction. Performances of SPWM and SVPWM modulations were evaluated under the same conditions in harmonics generation, by total harmonic distortion measurement, and the SVPWM method presented better results. On the other end, by increasing the number of vectors, this technique may be impracticable when acting with low cost conventional microprocessors. In both techniques, inverters dead times were realized in hardware, by dedicated integrated circuits, so that, besides avoiding crossed conductions, they didn't influence distortions.*

Keywords: *Inverter, Harmonics, SPWM, SVPWM.*

1. INTRODUCTION

Since some time, studies have been carried out for a three-phase induction motor to operate in high performance applications, including machines design changes so as to improve their characteristics, improve mathematical models to represent machines operation and, finally, with a significant number of published works, is the development of new algorithms and structures for drives control, realized in frequency control voltage inverters. Some of the subjects addressed in these works are scalar actuation, the field-oriented control method, as well as direct torque control. From the presented methods, the scalar is the one of easier implementation, whose proposal is to maintain constant flow (V / f = constant) (Lima et al. 2012).

The inverters are known as a type of electronic circuit converting direct current (DC) into alternate current (AC). The inverters are used in a variety of applications, such as: alternate current

(AC) power generation, UPS switches (Power Up Switch), variable frequency drives, three-phase machines control, high power transmitter applications (HVDC). Currently the inverters are based on high speed and power transistors, the most common of these being the isolated port, the IGBT and MOSFET.

These electronic keys are controlled by pulses of constant amplitudes and variable widths. Its control is made by a technique called pulse width modulation (PWM) that gave rise to several modulation techniques, among which are: modulation by hysteresis, harmonic elimination modulation (optimum MLP), sinusoidal modulation (SPWM), random modulation and vector space modulation (SVPWM). All, in one way or another, have contributed to the control of electric machines.

The modulation is the heart of the inverters and the choice of the model is a major problem in their design, since it determines the control greater or lesser reliability. The SPWM modulation technique is the most used since it is easy to implement and implies a low harmonics generation, when some recommendations are respected (Marcelino and Fiorotto 1999).

The SVPWM modulation technique may present advantages mainly in the control of three-phase induction motors (TIM), although due to computational complexity, this technique is almost always implemented by means of digital signal processors (Abood and Raheem 2014). SVPWM also has relevant attributes for a better performance of electric machines, among them: the reduction of the total harmonic distortion (THD), the linear operating range, the loss of Joule effect due to the switching dynamics of the electronic keys and the use more efficient DC voltage. The SVPWM seeks to determine the switches commuters' control, determining the time of the ON/OFF states, as a function of the instantaneous position of the reference vector (Loong 2008).

This work, through an exploratory research of these discrete realizations modulations, simulated the generation of signals specific to a TIM, using a PIC family microcontroller and confronted the results as a function of the harmonics generation.

The implementation of the SVPWM modulation in a low-cost microcontroller, opens the possibility of use in products with specific characteristics. The EXCEL program was used to calculate the equations variables and to generate the vectors. For the simulation, the PSIM and PROTEUS programs were used and, finally, the MATLAB was used as a support resource to confirm some results.

2. THREE-PHASE INVERTER

Three-phase induction motors, due to their constructive nature, present a relative difficulty for their control. Among the topologies of inverters for motor control are converters of two, three and five levels, all seeking the construction of an almost pure sine wave. This work was developed based on two levels topology, the simplest and easiest implementation. The two-level power converter circuit, as shown in Figure 1, is composed of a set of IGBT type electronic switches. These keys are controlled by six signals identified as *SW1* to *SW6*. However, only three of these are sufficient for control logic (Gaballah 2013).

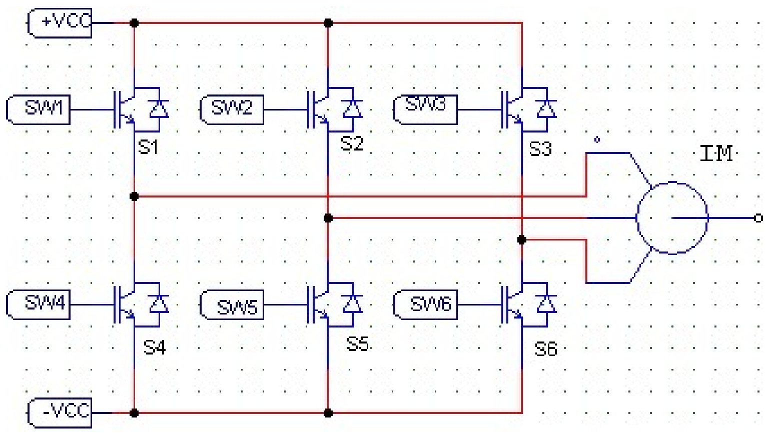

Figure 1. Illustration of two levels three-phase power circuit.

The most known modulation technique used for generating the circuit shown in Figure 1 control signals is SPWM. It is the result of comparison of three time discretized sine-wave signals, 120 ° apart, and a carrier signal, represented by a discretized triangular signal. Figure 2 shows the generation of a three-phase SPWM signal (*SW1*, *SW2* and *SW3*).

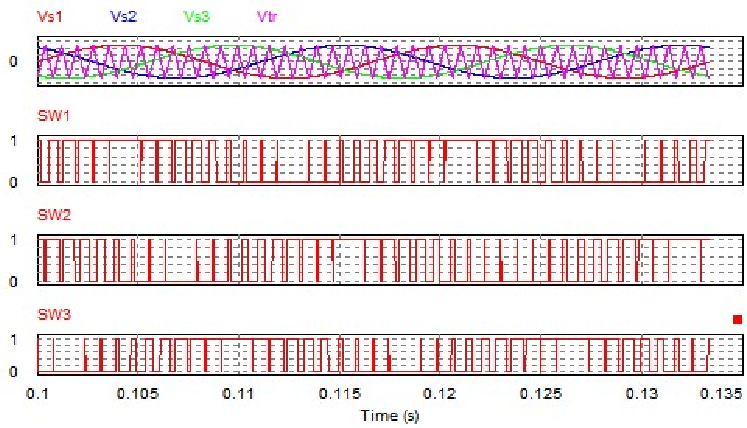

Figure 2. Generation of a three-phase SPWM signal.

According to Figure 2, the PWM signal can also be generated by another modulation method, SVPWM. It generates pulse width modulated pulses, directly at the processor output port, from a reference vector, for the periods construction (*Ts*), composed by eight sequentially chained signal segments, with times identified by: *Ta*, *Tb* and *Tc*. These times represent the signal permanence at high or low level in the construction of an octet. Figure 3 shows two typical periods of symmetric

SVPWM modulation.

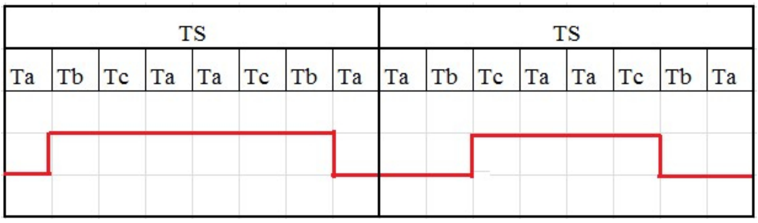

Figure 3. Two-period illustration of SVPWM signal (*Ts*).

2.1. SVPWM Technology

Three-phase induction motors operate when three sine signals are applied at their input terminals, out of phase with each other, as shown in Figure 4. The inverters seek to generate a signal pattern close to Figure 4 from a circuit, e.g. the type illustrated in Figure 1. The first step in generating the SVPWM for generating a switches low number, is to divide the Figure 4 signal period into points where at least two signals intersect, these points being adopted as the switching region, and, as a result, the period is divided into six sections, referred to as sectors (Wu et al. 2014). Figure 4 also shows this mapping.

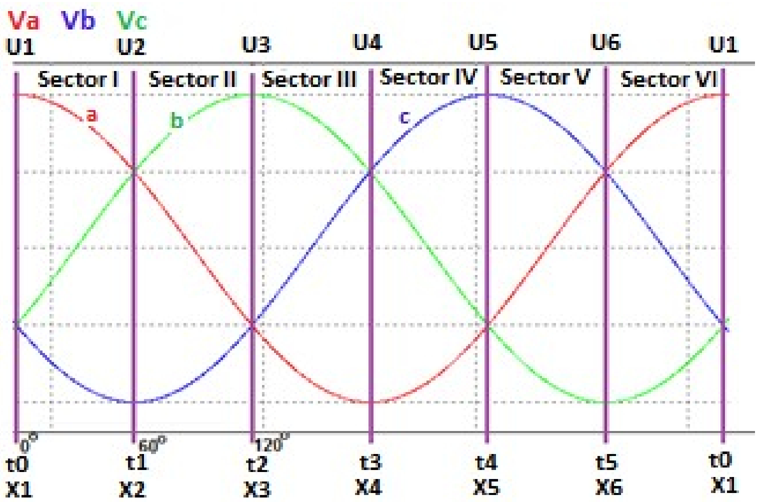

Figure 4. Three-phase sinusoidal signal divided into six sectors.

Figure 4 shows that there are six switching moments (*X1*, *X2*, ..., *X6*) within a period of a signal period, and they are associated with the power switches. The crossing points are spaced 60 degrees from each other. These points mark the beginning and the end of a particular sector, and each crossing point is associated with a state. Circuit of Figure 1 was simplified according to Figure 5 by changing the IGBT power switches by simple ON/OFF switches and the motor by resistive loads connected in a star configuration.

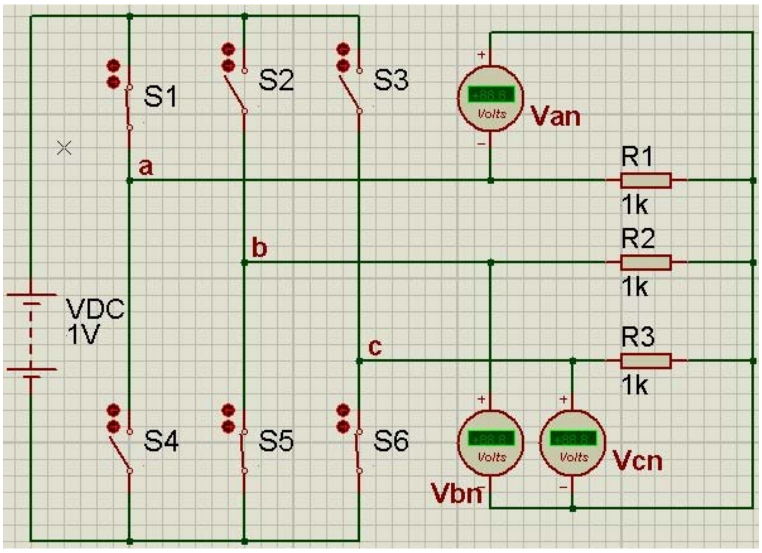

Figure 5. Two-level power circuit changed.

The lower switches are complementary to the upper ones, and this imposition makes it impossible that current occurs simultaneously between the switches *SW1*/*SW4*, *SW2*/*SW5* and *SW3*/*SW6*, avoiding a possible short circuit between the DC bus voltage and the GND. Effectively only the upper switches (*SW1*, *SW2*, *SW3*) allow for the generation of switching states. Total switching states are 23. Thus, there are only 8 possible configurations for the operations in a two-level conversion circuit. The circuit of Figure 5 was simulated in PROTEUS with all possible switching states and the result is presented in Table 1.

Table 1. Results of simulation of Figure 5.

States	*SW1*	*SW2*	*SW3*	*VaN*	*VbN*	*VcN*
0	0	0	0	0	0	0
1	1	0	0	+2/3	-1/3	-1/3
2	1	1	0	+1/3	+1/3	-2/3
3	0	1	0	-1/3	+2/3	-1/3
4	0	1	1	-2/3	+1/3	+1/3
5	0	0	1	-1/3	-1/3	+2/3
6	1	0	1	+1/3	-2/3	+1/3
7	1	1	1	0	0	0

It is seen that the maximum output voltage in a two-level system is (2/3) * Vcc (Pereira Filho 2007). This vectors mapping is characteristic of Six-Step type converters, presenting a low number of switches and, as a result, low switching losses are observed, desirable characteristics in any switched system. However, the output has a very high harmonic composition that can be minimized with the SVPWM switching technique (Kushwah and Wadhwani 2014).

2.2. SVPWM Technique Implementation

The SVPWM has the mission of generating a three-phase switched signal with characteristics very close to those of sinusoidal controllers and, to achieve such characteristics, it should have, among others: low harmonic distortion, low switching losses, extensive linear operating region Unlike the SPWM technique that generates the PWM signal, separately, by comparing each of three senoids, with a single (triangular) carrier signal, the SVPWM treats these sine signals as if they were a single signal, called the reference voltage (*Vref*). This reference signal contains the characteristics of the three sine-wave signals and must be represented at the output by the states variations of the switches (*SW1*, *SW2* and *SW3*) (Badran, Tahir, and Faris 2013).

Symmetrical three-phase induction motors present complex modeling due to the three phase lag of 120 ° (Figure 4). A transformation of this system to a two-phase system is possible by using the Clarke transform, which is a linear transform for three-phase systems. Actually, it transforms a symmetric three-phase machine (abc plane) into a symmetrical two-phase machine (plane where the *Vref* signal is generated, used in the SVPWM algorithm, with the advantages of maintaining constant the variables of torque, power and number of poles (Teixeira 2012). The Clarke transform can be applied analytically by Eq. (1) (Ponder and Pham 2015).

$$|Vref| = \begin{bmatrix} Vd \\ Vq \end{bmatrix} = \left(\frac{2}{3}\right) \cdot \begin{bmatrix} 1 & -1/2 & -1/2 \\ 0 & \sqrt{3}/2 & -\sqrt{3}/2 \end{bmatrix} \cdot \begin{bmatrix} Va \\ Vb \\ Vc \end{bmatrix} \quad (1)$$

Where: *Va*, *Vb* and *Vc* are the voltages in the abc plane and *Vd* (real) and *Vq* (imaginary) are the voltages transformed to the orthogonal plane).

Figure 6 shows the result of Clarke transform of a three-phase signal on a biphasic signal in the simulated time domain in MISP software.

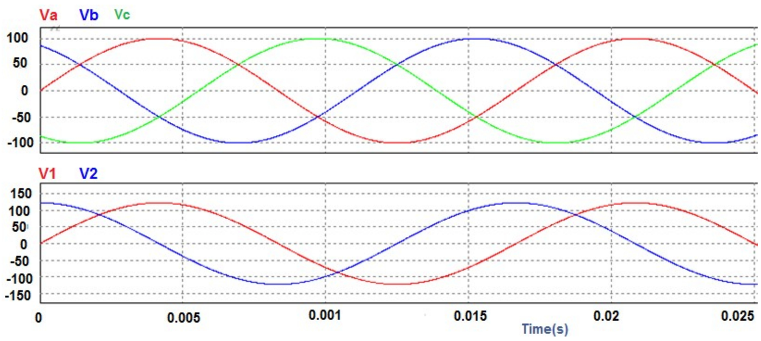

Figure 6. Three-phase signal converted to a two-phase signal.

The relationship between these planes is shown graphically as in Figure 7, where: Figure 7(A) shows the abc plane, and Figure 7(B) shows conjunction of plane abc, orthogonal plane and vector *Vref*.

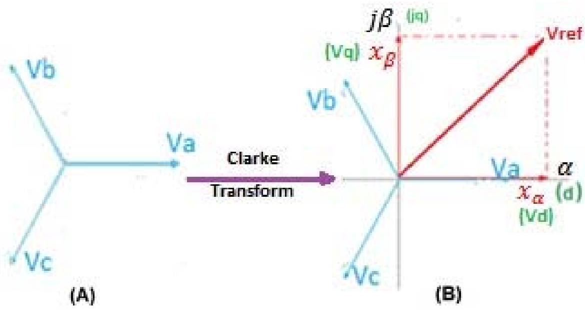

Figura 7. Vectors in plane abc and in plane αβ0 orthogonal) (Ponder and Pham 2015).

Figure 8 shows a diagram of vector space with the representation of six active vectors (*V1*, *V2*, *V3*, *V4*, *V5*, *V6*) as well as six sectors, each with a 60 º arc, completing a 360 º period. Each sector is a region between three vectors, two active and one null, where vector Vref rotates at a constant velocity across all sectors for the generation of the output sinusoidal signal. According to Figure 8, there is a direct relationship between time *T1* of vector *V1* and *T2* of vector *V2* and voltage *Vref*. This relation is expressed in Eq. (2).

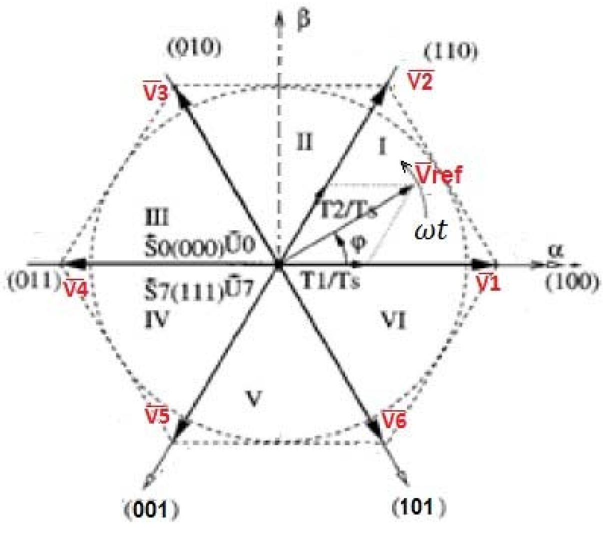

Figure 8. Vector space (hexagonal plane) with the respective sectors and *Vref* (Abood and Raheem 2014).

$$|Vref| = \left(\frac{T1}{Ts}\right)|V1| + \left(\frac{T2}{Ts}\right)|V2| \tag{2}$$

Where:

Ts is the PWM switching period;

T1 = duration of time on a vector of sector x (x = I to VI);

T2 = time duration over the other sector vector x.

This relation holds for all other vectors (changing the vectors indices). The residence times of signals *T1*, *T2* and *T0* of the state vectors are related to the signals. Equations (3), (4) and (5) allow for the computation of these times (Lakhimsetty et al. 2014).

$$T1 = \sqrt{\frac{3}{2}} \cdot m \cdot Ts \cdot \sin\left[n \cdot \left(\frac{\pi}{3} \right) - \phi \right] \tag{3}$$

$$T2 = \sqrt{\frac{3}{2}} \cdot m \cdot Ts \cdot \sin\left[\phi - (n-1) \cdot \frac{\pi}{3} \right] \tag{4}$$

$$T0 = Ts - T1 - T2 \tag{5}$$

Equations (3) and (4) can be rewritten as:

$$T1 = K \cdot \sin\left[n \cdot \left(\frac{\pi}{3} \right) - \phi \right] \tag{6}$$

$$T2 = K \cdot \sin\left[\phi - (n-1) \cdot \frac{\pi}{3} \right] \tag{7}$$

where:

$$K = \sqrt{\frac{3}{2}} \cdot m \cdot Ts \tag{8}$$

Where:

n = sector number (1 ... 6);

Ts = time of the SVPWM period;

$\sqrt{3/2}$ = angle of rotation of vector *Vref*, and

m = modulation index, given by $Vref/Vdc$.

Equations (3) and (4) were rewritten to obtain a static part (*K*), which defines the output signal characteristics, and a dynamic part, which determines the normalized amplitude as a function of rotation of vector *Vref*.

The value of period (*Ts*) of the SVPWM signal is computed by Eq. (9).

$$Ts = \frac{1}{Np \cdot f} \tag{9}$$

where:
Np is the number of Ts periods;
f is the frequency given in Hertz.

2.3. SVPWM Strategy Modulation

According to Figure 8 it is seen that vector *Vref* rotates at a constant speed through the sectors: sector I (*V1*-*V2*); sector II (*V2*-*V3*); sector III (*V3*-*V4*); sector IV (*V4*-*V5*); sector V (*V5*-*V6*) and sector VI (*V6*-*V1*). Each sector operates with a conventional switching sequence, and Figure 9 shows that of sector I.

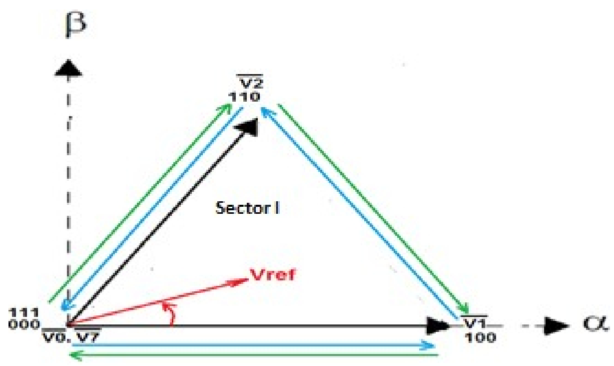

Figure 9. Sector I conventional switching sequence.

Sector I conventional switching sequence takes place in two steps, the first indicated by the blue arrow, originating from vector 0 (null) and destination in vector 7 (null) and then indicated by the green arrow, originating from vector 7 and destination in vector 0. This sequence generates eight sequential switch vectors that are presented in Table 2.

Table 2. Switching vectors according to sector I.

	Time	***t0***	***t1***	***t2***	***t3***	***t4***	***t5***	***t6***	***t7***
Sector I	Vectors	000	100	110	111	111	110	100	000

Applying the sequential switching to the remaining sectors, the switching vectors shown in Table 3 were generated.

Table 3. Sectors II to VI switching vectors.

	Time	***t8***	***t9***	***t10***	***t11***	***t12***	***t13***	***t14***	***t15***
Sector II	**Vectors**	000	010	110	111	111	110	010	000
	Time	***t16***	***t17***	***t18***	***t19***	***t20***	***t21***	***t22***	***t23***
Sector III	**Vectors**	000	010	011	111	111	011	010	000
	Time	***t24***	***t25***	***t26***	***t27***	***t28***	***t29***	***t30***	***t31***
Sector IV	**Vectors**	000	001	011	111	111	011	001	000
	Time	***t32***	***t33***	***t34***	***t35***	***t36***	***t37***	***t38***	***t39***
Sector V	**Vectors**	000	001	101	111	111	101	001	000
	Time	***t40***	***t41***	***t42***	***t43***	***t44***	***t45***	***t46***	***t47***
Sector VI	**Vectors**	000	100	101	111	111	101	100	000

Times *t0* to *t47* are specific sequence events for six vector sets (*Np* = 6) SVPWM modulation. The switch vector information, according to Tables 2 and 3, can be represented in the switches / sectors state diagram Figure 10 shows this representation.

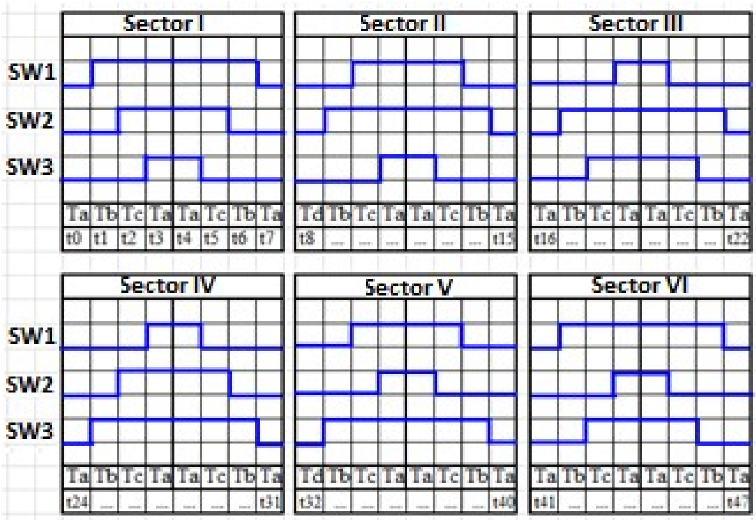

Figure 10. States diagram (Loong 2008).

Times *Ta*, *Tb* and *Tc* are permanent times of each switching vector on the switches. These times are computed according to Eqs. (3) to (8), applied in the respective sectors (I to VI) where $Ta = T0/4$, $Tb = T1/2$ and $Tc = T2/2$. Times *T0*, *T1* and *T2* may have the same or different values, and they are obtained from the magnitude and relative position of the *Vref* vector in the orthogonal plane (Rahman et al. 2013; Yu 1999).

2.4. Output Signal Quality

The level of harmonic distortion of the output signal is directly related to the number of pulses of the SVPWM signal per period of the output signal, identified in this work by *Np*. A smaller number of *Np* implies an output signal with a higher number of harmonics coupled to the signal and vice versa. It indicates the number of positions that the reference vector has in the hexagonal space, known as reference vector parking positions. Due to the constant rotation velocity of vector *Vref*, these discrete points are equidistant from each other, and this distance is expressed by an angle identified in this work by $\hat{A}$, determined by Eq. (10).

$$\hat{A} = \frac{2\pi}{Np} \tag{10}$$

where: $Np \geq 6$ to ensure at least one representation per sector.

Depending on the value chosen for *Np*, which determines the vector *Vref* displacement angle, values of *T0*, *T1* and *T2* can be repeated in all sectors, as shown in Table 4.

Table 4. *K*, *T1*, *T2* e *T0* computed values.

Angle(degrees)	**Angle (radians)**	**Sectors (*n*)**	***T1* (µs)**	***T2* (µs)**	***T0* (µs)**
15	0.2617	1	425	156	808
45	0.7853	1	156	425	808
75	1.3089	2	425	156	808
105	1.8325	2	156	425	808
135	2.3561	3	425	156	808
165	2.8797	3	156	425	808
195	3.4033	4	425	156	808
225	3.9269	4	156	425	808
255	4.4505	5	425	156	808
285	4.9741	5	156	425	808
315	5.4977	6	425	156	808
345	6.0213	6	156	425	808

3. SIMULATIONS AND RESULTS

The aim of this article is to apply all previously presented concepts on the SVPWM modulation, through simulation of for three-phase induction motor controller, using a microcontroller of the PIC18F452 family, measuring the total harmonic distortion and confronting with an SPWM controller, under the same load conditions and with the same number of SVPWM periods.

3.1. Three-Phase Inverter with SVPWM Modulation

A PIC18F452 microcontroller operating at 40 MHz, reset circuit, a three-phase two-level power circuit with six switches, an inductive load, simulating the motor, and a differential circuit to measure current in the load, and two oscilloscopes, were inserted into the PROTEUS software oscilloscopes.

3.2. Definition of Inverter Characteristics

a) m = 50 % (modulation index);
b) f = 60 Hz (output signal frequency);
c) Np = 12 (SPWM signal number of periods (Ts) for a period (T) of output signal). The value Np = 12 was not larger that the $T0$, $T1$ and $T2$ values, and were not too small, which would require faster processing.

3.3. Computations of Reference Vector Parking Positions

The reference vector displacement angle $\hat{A}$ is obtained from Eq. (10):

$$\hat{A} = 0.5236 \text{ rd or } 30.$$

Figure 11 shows the resulting hexagonal plane.

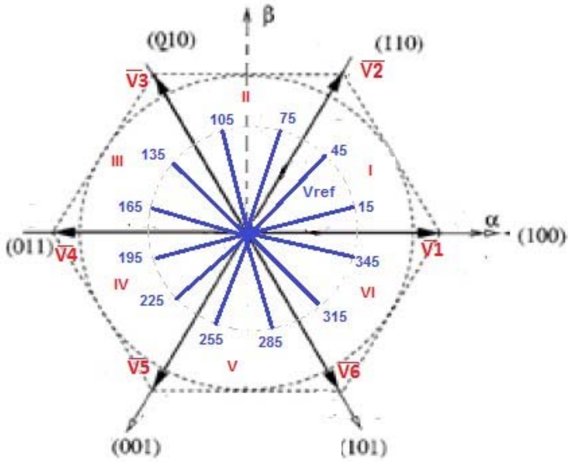

Figure 11. Hexagonal plane with the reference vectors positions for *Np* = 12.

3.4. SVPWM Signal Period and Times Computation

The period is computed from Eq. (9):

$$Ts = \frac{1}{720}\ [s].$$

From Eqs. (3), (4) and (5), it was possible to calculate times *T1*, *T2* and *T0* with the following input data: *Vdc* = 10 V, *Vref* = 5 V, *f* = 60 Hz and *Np* = 12. Results are given in Table 4.

It is noted according to Table 4, that inside a sector times *T0*, *T1* and *T2* have different values as a function of displacement of the *Vref* vector. As shown in Figure 11, the *Vref* vector moves in sector I by 15 º and 45 º. The same values of *T0*, *T1* and *T2* of sector I are used in sectors II through VI, because the angular displacement of vector *Vref*, in each sector, presents the same relative displacement, otherwise this repetition would not occur.

3.5. PROTEUS SVCPWM Simulation

In order to control the circuit designed in PROTEUS, a software was written in C language, and the parameters of Table 4 were inserted into the program in the form of a search table. After the simulation, the output waveforms are presented according to Figure 12.

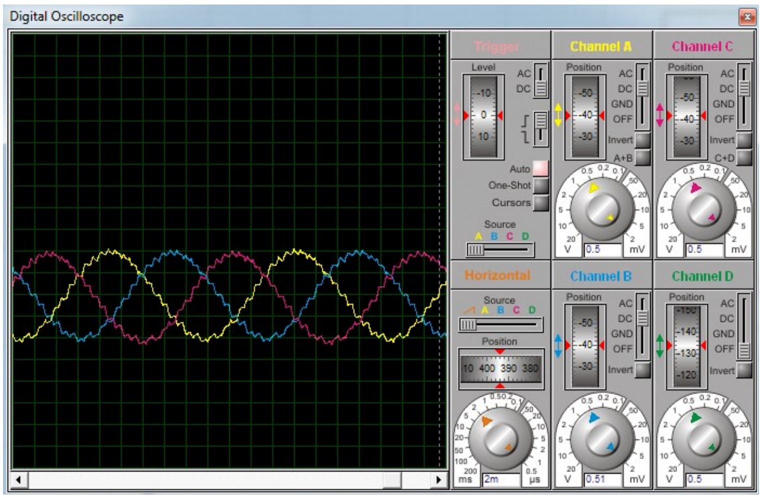

Figure 12. Output of SVPWM controller for 12 periods of SVPWM signal.

It is noted that, added to its fundamental, the three-phase signal presents a harmonic distortion. After an analysis in the frequency domain of this signal, the spectral result is presented in Figure13.

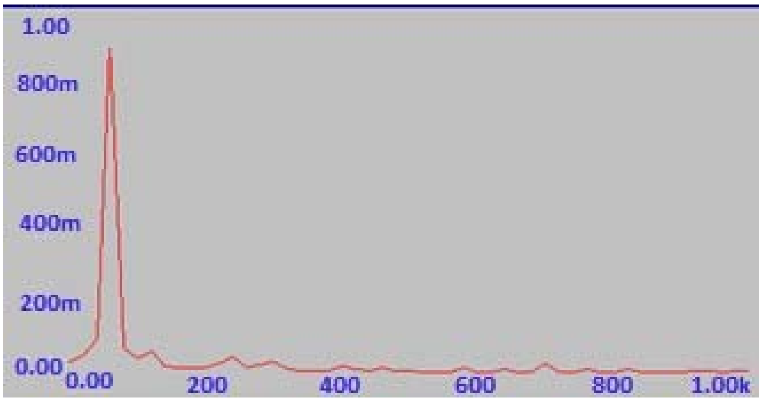

Figure 13. Figure 12 signal frequency spectrum.

The value of total harmonic distortion, relative to Figure 13 is a THD of 3.4 %.

3.6. A Three-Phase Inverter SPWM Simulation

The circuit designed in PROTEUS has been changed to generate SPWM pulses for the control of *SW1*, *SW2* and *SW3* switches. The microcontroller was removed, three sinusoidal generators set at 60 Hz were inserted, by 120 º displaced phases and a triangular generator set at 720 Hz. These were compared to generate three pulsed SPWM signals, which were injected into the switches. These values were required to be compatible with the SVPWM modulation, with Np = 12. All other parameters are also compatible. The simulation process in PROTEUS was triggered and the circuit generated three alternating and 120 º lagged waves. Figure 14 shows the result of simulation.

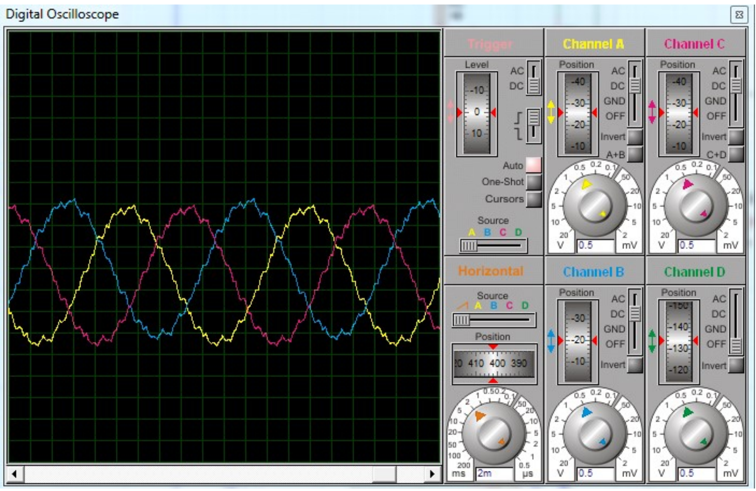

Figure 14. Output of the SPWM controller.

From Figure 14 it is noted that, added to its fundamental, the three-phase signal has a harmonic distortion. After an analysis of this signal in the frequency domain, the resulting spectrum is shown in Figure 15.

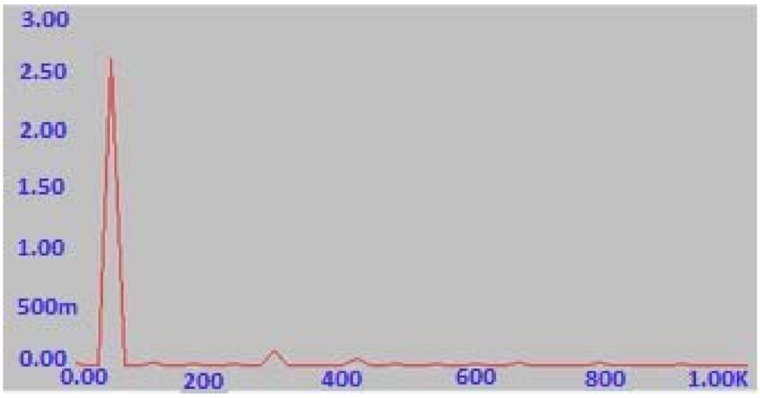

Figure 15. Figure 14 Signal frequency spectrum.

The total value of harmonic distortion, relative to Figure 15, is a THD of 5.33 %.

It is concluded that for the same operating conditions, that is, 60 Hz fundamental frequency, same load and equivalent sampling frequency, the SVPWM modulator THD presented a lower value than the SPWM modulator THD.

3.7. New Output Signal Settings

In order to generate other output signal frequencies, the *T0*, *T1* and *T2* values should be changed. The amplitude may be altered by the variation of the modulation index and, when necessary, to further decrease the THD and the value of *Np* should be changed (18, 24, 30 ....). As a result, new values of *T0*, *T1* and *T2*, relative to each position of vector *Vref*, are obtained, but the computational load may be infeasible for a conventional microcontroller when these changes are constant in the process, which justifies the application of this technique by always using digital signal processors.

3.8. Activating an TIM at 60 Hz

The TIM drives with the SVPWM and SPWM modulations were simulated, configured so that the harmonic noise generated in the power grid was similar in both modulations. Thus, it was necessary to configure the SVPWM with *Np* = 24, which resulted in two preprogrammed tables with a total of 112 bytes. SPWM, peer-to-peer, required a total of 756 bytes in the preprogrammed table. Both tables were generated using two programs written in C language and later run on a low cost microcontroller, the PIC18F4550. The final result was:

a) The ability to rotate an TIM at 60 Hz, by both modulations;
b) The SVPWM table had 14.81 % of the SPWM table size;
c) SVPWM has made the microcontroller performance of low cost more efficient, by acting only in the moments of effective decisions.

4. CONCLUSIONS

SVPWM modulation is a predominantly digital algorithm, requiring continuous computations, since it manipulates very small and variable times, requiring high processing capacity. This explains why this technique has only recently been used, mainly due to the advancement of processors and microcontrollers technology, where processing time has greatly decreased, opening the way to new modulation techniques. SPWM technique can be implemented, both analogously and digitally, with the analog form being preferred for simulations, due to the profile of PSIM simulators. EXCEL, PSIM, MATLAB and PSIM tools helped at various stages of this work. MATLAB was useful in functions calculation, EXCEL allowed for the creation of tables to determine the values of *T1*, *T2* and *T0*, and PSIM software provided a view of the behavior of Clarke transform graphic. PROTEUS simulator was an indispensable tool for simulating SVPWM algorithm in a two-level circuit, allowing visualization of output waveforms, as well as making an output signal spectral analysis. Performances of SPWM and SVPWM modulations were measured under the same conditions and, in a specific case, in harmonics generation, through THD measurement, and SVPWM presented better results. Even with greater computational requirements, its use in motor controllers, for specific loads and without major changes, may have satisfactory results, with discrete switches signals being pre-programmed in search tables, in low cost microcontrollers.

The activation of an TIM at 60 Hz by both modulations, using pre-programmed tables, showed that the SVPWM occupies 85.16 % less memory area for the tables, requiring less processing capacity of the microcontroller, since it only acts on the electronic keys in the effective decision moments and, consequently, more processing time remaining for the other tasks.

The use of pre-programmed tables reduced the processing load of SVPWM modulation, commonly used only in digital signal processors, with high processing capacity but with equally high costs.

REFERENCES

Abood, Sameer Ibraheem, and Mohammed Sabri A. Raheem. 2014. “Performance Analysis of SPWM and SVPWM Inverters Fed Induction Motor.” *International Journal of Computer Applications* 86 (5): 33–38.

Badran, Marwan A. A., Ahmad M. Tahir, and Waleed F. Faris. 2013. “Digital Implementation of Space Vector Pulse Width Modulation Technique Using 8-Bit Microcontroller.” *World Applied Sciences Journal* 21: 21–28. https://doi.org/10.5829/idosi.wasj.2013.21.mae.99945.

Gaballah, Mahmoud M. 2013. “Design and Implementation of Space Vector PWM Inverter Based on a Low Cost Microcontroller.” *Arabian Journal for Science and Engineering* 38 (11): 3059–70. https://doi.org/10.1007/s13369-012-0464-2.

Kushwah, S., and Arun K. Wadhwani. 2014. “Space Vector Pulse Width Modulation for a Two-Level VSI Using MATLAB.” *International Journal of Engineering Research and Applications*, no. ICETMEE: 180–84.

Lakhimsetty, Suresh, Mahesh K., Janardhna M., and Mahesh M. 2014. “Simulation of Space Vector Pulse Width Modulation for Voltage Source Inverter Using MatLab/Simulink.” *Journal of Automation & Systems Engineering* 8 (3): 133–40.

Lima, Fabio, Walter Kaiser, Ivan Nunes da Silva, and Azauri Albano de Oliveira. 2012. “Speed Neuro-Fuzzy Estimator Applied To Sensorless Induction Motor Control.” *IEEE Latin America Transactions* 10 (5): 2065–73. https://doi.org/10.1109/TLA.2012.6362350.

Loong, Kelvin Lye Kwong. 2008. “Micro-Controller Based Space Vector Modulation (SVM) Signal Generator.” Malaysia: Universiti Teknologi Malaysia.

Marcelino, Márcio Abud, and F. A. Fiorotto. 1999. “Geração Para Controle de Velocidade de Motores - PI-9704081-9.” *Revista Da Propriedade Industrial* 1470: 1–9.

Pereira Filho, Nicolau. 2007. “Técnicas de Modulação Por Largura de Pulso Vetorial Para Inversores Fonte de Tensão.” Universidade Federal de Itajubá.

Ponder, Aaron, and Long T. Pham. 2015. “Space Vector Pulse Width Modulation in Wind Turbines Generator Control.”

Rahman, Ahmad Shukri Fazil, Muzaidi Othman Marzuki, Abdul Rahim Abdul Razak, Syafruddin Hasan, Baharuddin Ismail, and Syed Idris Syed Hassan. 2013. "Microcontroller Based SPWM Generator: A Conventional Design Perspective Through Graphical Oriented Approach." *International Journal of Innovative Technology and Research* 1 (3): 226–32.

Teixeira, D. C. N. 2012. "Controle Vetorial Do Motor de Indução Operando Na Região de Enfraquecimento de Campo." Universidade Federal de Viçosa.

Wu, Yuan-Kang, Yuan-Hao Yang, Huei-Jeng Lin, and Shih-Yu Yang. 2014. "Modelling and Control of a Small Wind Turbine by Using PSIM." In *2014 CACS International Automatic Control Conference (CACS 2014)*. Wu2014: IEEE. https://doi.org/10.1109/CACS.2014.7097168.

Yu, Zhenyu. 1999. "Space-Vector PWM With TMS320C24x/F24x Using Hardware and Software Determined Switching Patterns: Application Report SPRA524." Dallas, TX.